JACS
JOURNAL OF THE AMERICAN CHEMICAL SOCIETY

COMMUNICATION

pubs.acs.org/JACS

Cellular Uptake Mediated Off/On Responsive Near-Infrared Fluorescent Nanoparticles

Aniello Palma,[†] Luis A. Alvarez,[‡] Dimitri Scholz,[‡] Daniel O. Frimannsson,[†] Marco Grossi,[†] Susan J. Quinn,[†] and Donal F. O'Shea*[,†]

[†]Centre for Synthesis and Chemical Biology, School of Chemistry and Chemical Biology, University College Dublin, Belfield, Dublin 4, Ireland

[‡]UCD Conway Institute, University College Dublin, Belfield, Dublin 4, Ireland

Supporting Information

ABSTRACT: Fluorescence imaging, utilizing molecular fluorophores, often acts as a central tool for the investigation of fundamental biological processes and offers huge future potential for human imaging coupled to therapeutic procedures. An often encountered limitation with fluorescence imaging is the difficulty in discriminating nonspecific background fluorophore emission from a fluorophore localized at a specific region of interest. This limits imaging to individual time points at which background fluorescence has been minimized. It would be of significant advantage if the fluorescence output could be modulated from *off* to *on* in response to specific biological events as this would permit imaging of such events in real time without background interference. Here we report our approach to achieve this for the most fundamental of cellular processes, i.e. endocytosis. We describe a new near-infrared *off* to *on* fluorescence switchable nanoparticle construct that is capable of switching its fluorescence on following cellular uptake but remains switched off in extracellular environments. This permits continuous real-time imaging of the uptake process as extracellular particles are nonfluorescent. The principles behind the fluorescence off/on switch can be understood by encapsulation of particles in cellular organelles which effect a microenvironmental change establishing a fluorescence signal.

The use of organic fluorophores as *in vitro* reporters of dynamic biological and environmental processes is ubiquitous in molecular and cell biology research programs. The recent technological advances in noninvasive small animal fluorescence imaging and the future prospect of routine human fluorescence imaging have given rise to a resurgent interest in suitable molecular fluorophores which have emission in the near-infrared (>700 nm) spectral region.[1] Their simplicity of use, coupled with high sensitivity, ensures a continual expansion of their applications for *in vitro* and *in vivo* imaging.[2−5] While several new classes of molecular NIR probes are currently emerging[6−8] the opportunity exists to develop a superseding next generation of smart fluorescent probes which have both the optimal photophysical characteristics and the ability of switching their fluorescence signal from off to on in response to specific biological stimuli.[9,10]

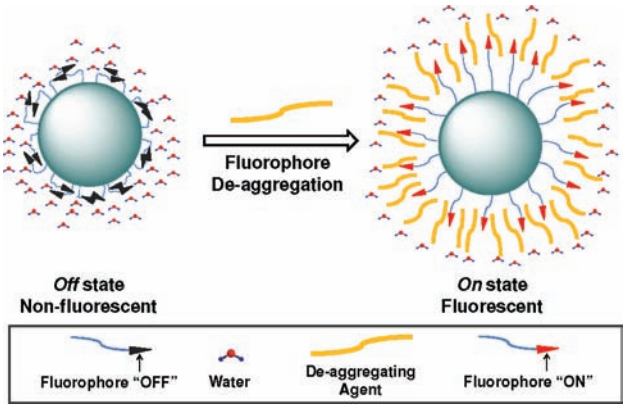

Figure 1. Switching mechanism design for off/on fluorescent nanoconstructs.

If fluorophores could be engineered to remain fluorescent silent and only be activated in recognition of a specific biological event this would provide a huge signal-to-noise ratio in the targeted area and minimize background fluorescence. This would open the way to continuous real-time imaging rather than acquiring single time point static images following clearance of a nonspecific fluorophore (either by washing for *in vitro* cells or natural clearance *in vivo*).

Fluorophore immobilization on or within particles can yield significant photophysical benefits and is being increasingly investigated for roles in nanomedicine, nanobiotechnology, and fluorescence imaging.[11,12] Recently, the advent of particle-based fluorophores has focused on noncovalently linked dye-doped polymer particles. In contrast, the development of particles with surface covalently bound fluorophores is far more limited. A potential advantage of covalently linking the fluorophores at the surface of a particle is that they may be induced to respond to stimuli in the surrounding microenvironment as they are not shielded by a surrounding particle. Therefore the engineering of surface modified fluorescent nanoparticles which can act as a responsive fluorescent imaging agent represents a worthwhile pursuit (Figure 1).

In this report we outline the design, synthesis, characterization, and *in vitro* illustration of a cellular uptake activated off to on switchable fluorescent nanoparticles. The switching mechanism

Received: August 26, 2011
Published: November 10, 2011

dx.doi.org/10.1021/ja208086e | *J. Am. Chem. Soc.* 2011, 133, 19618–19621

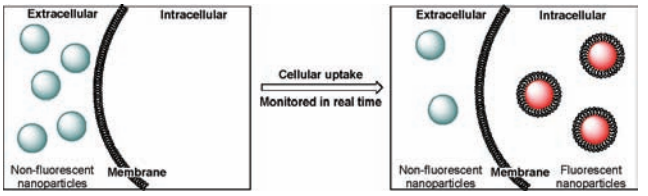

Figure 2. Schematic of cellular uptake controlled off/on fluorescent nanoparticle switching.

is based on the control of molecular fluorophore aggregates at the particle surface.[13] The particle off state (nonfluorescent) is engineered in aqueous environments by excited state quenching due to hydrophobic fluorophore aggregation (Figure 1, off state). Yet in the presence of a micelle forming deaggregating agent the individual fluorophore molecules would be able to relax away from the surface of the particle and be shielded from the surrounding water molecules thereby giving rise to a large enhancement of their fluorescence intensity (Figure 1, on state).

Our first anticipated biological application was to use these nanoparticle constructs for continuous live imaging of their cellular uptake. Effective visualization of this process in real time requires extracellular nanoparticles to have low fluorescence intensity, due to the quenching effects described above, but upon uptake into cells the particles would be surrounded by cellular vesicles such as endosomes which would turn on their fluorescence (Figure 2). While many different cellular uptake mechanisms for particles exist, a common feature is their encapsulation within a cellular vesicle upon uptake which could effect a microenvironmental change and cause the fluorescence to be switched on. This approach would eliminate background fluorescence and permit continuous imaging of the internalization of particles in the presence of nonfluorescent extracellular particles.

In order to build such a responsive nanoconstruct, our particles of choice were poly(styrene-*co*-methacrylic acid) polymers which have a defined high loading of surface carboxylic acid functional groups available for synthetic transformations. For ease of handling a 200 nm diameter particle size was selected for this initial study. As it is strongly preferential to image in the near-infrared spectral region, the BF_2 chelated tetraarylazadipyrromethenes were selected as fluorophores as they have a strong emission at ~725 nm.[8,10] Hydrophobic fluorophores were chosen as they would be effectively quenched in an aqueous environment especially at high loadings on the particle surface. Two different BF_2 chelated azadipyrromethenes **1a**, **b** were used differing only by the inclusion of a short polyether group attached to one aryl ring in **1b** instead of a methoxy group as in **1a** (Scheme 1). It was anticipated that the polyether substituent may impart subtle differences in the cellular uptake of the particles.[14]

Our synthetic approach started with particles NP_{COOH} which were converted into their corresponding activated esters NP_{Ester} by reaction with *N*-hydroxysuccinimide (NHS) and 1-ethyl-3-(3-dimethylaminopropyl)carbodiimide (EDCI) at rt (Scheme 1). Reaction of NP_{Ester} with fluorophores **1a** and **1b** yielded the corresponding nanoparticles NP**1a** and NP**1b** respectively (Table 1). Particles were purified by passing through C-18 reversed phase silica eluting with water which effectively removed any noncovalently linked fluorophore.

The zeta potential of the starting nanoparticles NP_{COOH} was measured at −62.9 mV (Table 1, entry 1) whereas following

Scheme 1. Synthesis of NP1a and NP1b

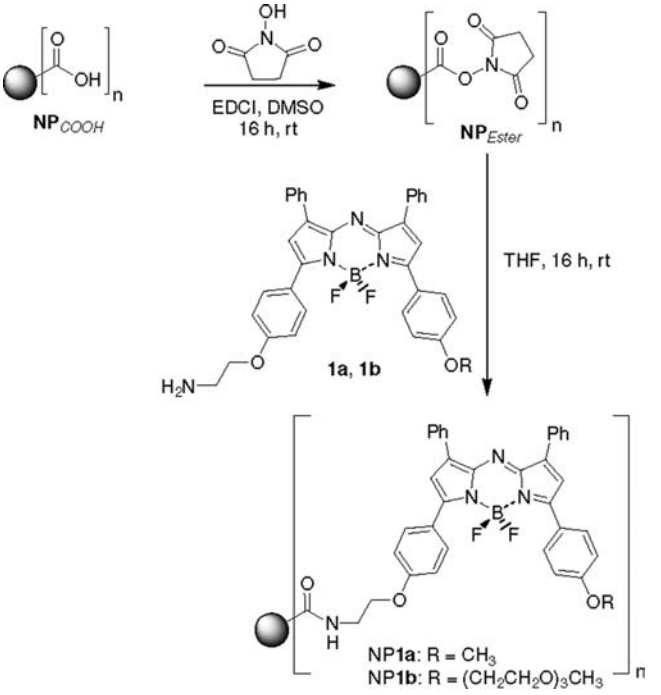

Table 1. Characterization of NP_{COOH}, NP1a, and NP1b[a]

entry	nanoparticle[a]	zeta potential (mV)	particle size/ H_2O	particle size/ H_2O + TX-100
1	NP_{COOH}	−62.9	205 ± 0.5	–
2	NP**1a**	9.4	198 ± 3	217 ± 6
3	NP**1b**	−11.2	199 ± 1	272 ± 19

[a] Concentration 0.001% w/w in HPLC grade water.

Table 2. Characterization of NP1a and NP1b

		λ_{max} emission (nm)[a]			
entry	NP	toluene	PBS	PBS+TX-100[b]	FEF[c]
1	NP**1a**	717	717	723	16
2	NP**1b**	718	720	725	11

[a] Concentration of 0.01 mg/mL. [b] Solution of TX-100 in PBS (0.34 mM). [c] Emission peak area in PBS+TX-100 (0.34 mM)/emission peak area in PBS.

functionalization with the neutral fluorophores the surface charge was dramatically altered. NP**1a** and NP**1b** gave measured zeta potentials of +9.4 and −11.2 respectively which indicates that the majority of surface carboxylic acids had been reacted and the particle surface had become relatively uncharged (Table 1, entries 2, 3). Analysis of the nanoparticles emission profiles in organic solvents such as toluene showed them to be highly fluorescent with λ_{max} values close to that of their corresponding molecular fluorophores (Table 2, Supporting Information (SI)).[8] In aqueous media such as phosphate buffered saline (PBS), as predicted, the fluorescence was dramatically quenched but with little change in λ_{max} of emission (Figure 3, Table 2).

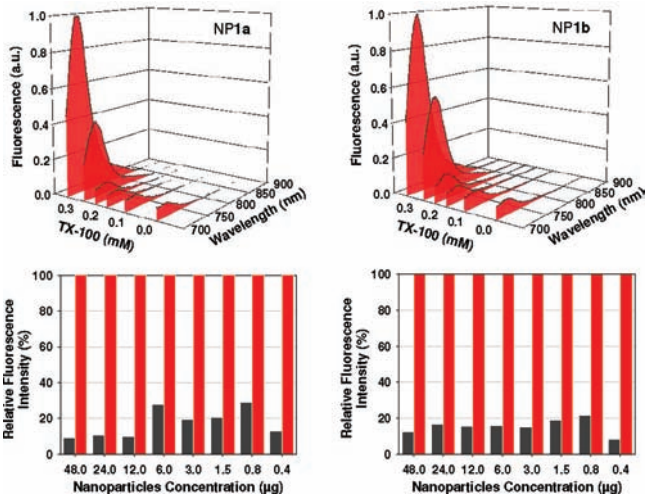

Figure 3. Top: Incremental titration of NP**1a, 1b** with TX-100 in PBS. Bottom: Normalized fluorescence intensity difference of NP**1a** and NP**1b** in Dulbecco's media + 10% FCS (gray), Dulbecco's media/TX-100 (red) at particle concentrations of 48, 24, 12, 6, 3, 1.5, 0.75, and 0.375 μg/well (each well contains 300 μL of media).

In contrast, when the nonionic surfactant Triton X-100 (TX-100) was added the fluorescence intensities were dramatically increased with a fluorescence enhancement factor (FEF) of 16 and 11 recorded for NP**1a** and NP**1b**, respectively (Table 2, Figure 3, SI). Such high FEF values indicate a very effective switching mechanism. In contrast, particle equilibration with bovine serum albumin (0.1 mM) for 2 h gave rise to a relatively small fluorescence increase (SI).

A similar increased fluorescence response was observed following the addition of the anionic surfactant sodium dodecylsulphate (SDS) and the phospholipid L-α-phosphatidylcholine (SI). The latter was particularly encouraging as phosphatidylcholines are a class of phospholipids that are a major component of biological membranes. Most interestingly, when TX-100 was added incrementally to a PBS solution of NP**1a** or NP**1b** the fluorescence intensity remained relatively unchanged until the critical micelle concentration (CMC) range of TX-100 (0.19−0.30 mM) (Figure 3).[15] This illustrates that it is not a linear fluorescence response to the TX-100 but rather a response to a particle−surfactant interaction initiating at the CMC.[16]

In order to probe this further additional characterization of these systems was undertaken using dynamic light scattering (DLS). DLS analysis showed that the starting and fluorophore functionalized particles NP_{COOH}, NP**1a** ,and NP**1b** were monodispersed as individual particles in water giving a measured diameter size of 205, 198, and 199 nm, respectively (Table 1). Revealingly, upon the addition of TX-100 to the three particle types the measured diameter size of NP_{COOH} did not change, yet NP**1a** and NP**1b** increased to 217 and 272 nm, respectively. This increase of diameter for the hydrophobic fluorophore functionalized particles is indicative of a close association of TX-100 around the particle.

As it could be readily envisaged that this off to on switching parameter could be exploited in a diagnostic assay format, the detection limit of the switching NP**1a** and NP**1b** in Dulbecco's cell growth media supplemented with 10% FCS (fetal calf serum) (with and without TX-100) was determined using a 96-well plate reader. The fluorescence intensities from a serial dilution of

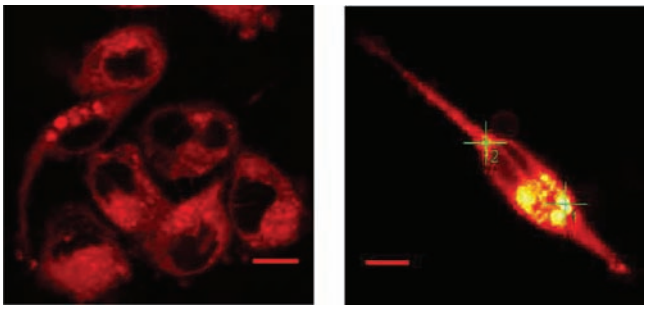

Figure 4. Left: Static fluorescence images of MDA-MB-231 cells with NP**1b** following 2 h of incubation, washing, and mounting of cells (scale bar 10 μm). Right: Single cell image; see SI for Z-stack images and emission spectra taken from points within the cell.

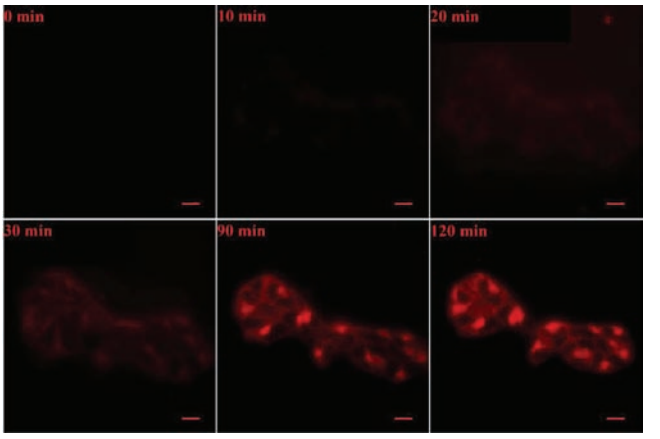

Figure 5. Real-time fluorescence imaging of NP**1b** uptake into HEK293T cells (scale bar 10 μm) (see SI for movie).

nanoparticles from 48 to 0.375 μg of nanoparticle per well in both their off and on states were recorded. Encouragingly, it was possible to obtain plate readable differences at each concentration level (Figure 3, bottom).

Based on these findings, NP**1b** was investigated for its potential as a real time *in vitro* imaging agent using MDA-MB-231 (breast cancer), HEK293T (kidney), and CAKI-1 (renal cancer) cell lines. Our aspiration was that the process of cellular endocytosis of NP**1b** would induce the off to on switching of the particles in a manner observed with surfactants. Initially, a single time point confocal imaging of NP**1b** using MDA-MB-231 cells was investigated. NP**1b** and cells were coincubated for 2 h, and the cells were washed, mounted on a glass slide, and imaged. Encouragingly the cells were highly fluorescent illustrating that the particles were effectively uptaken and highly fluorescent within the cells (Figure 4).

Real time imaging was next attempted using HEK293T and CAKI-1 cells as examples. The fact that extracellular NP**1b** particles are virtually fluorescent silent in cell growth media allowed the particles and cells to be coincubated together without a masking fluorescent signal.

Following addition of particles to the cell culture chamber, fluorescence images were acquired at short time intervals (to suit the rate of uptake) and compiled into a real-time movie of the uptake process. For HEK293T cells, images were acquired every 60 s for 120 min (see SI for movie). In Figure 5 six static frames of

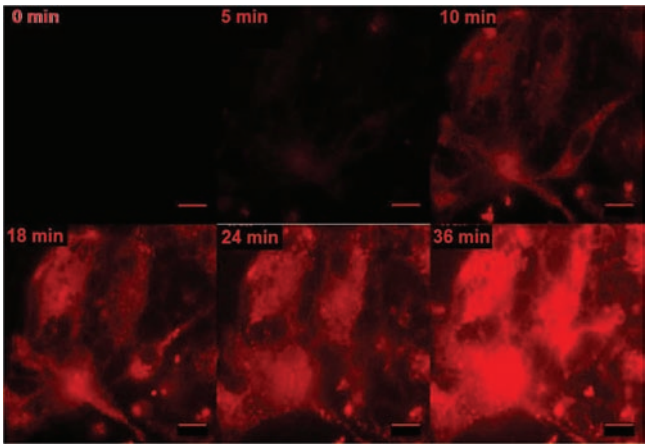

Figure 6. Real-time fluorescence imaging of NP**1b** uptake into CAKI-1 cells (scale bar 10 μm) (see SI for movie).

the uptake imaging of HEK293T cells with NP**1b** are shown in which it is clear that the fluorescence intensity increases over time as the particles are uptaken but also that the extracellular particles are relatively nonfluorescent (dark background). Over the 2 h time period the particle fluorescence can be clearly seen to pass through an initial diffuse pattern to concentrate in the perinuclear region.

In the case of CAKI-1 cells, uptake occurred more rapidly so images were acquired every 20 s for 30 min. In this case a rapid cellular uptake could again be observed culminating in the dramatic cell death of individual cells (Figure 6; see SI for movie).

The real-time observation of these cellular events clearly illustrates the potential of this imaging approach.

In conclusion, a synthetically robust and efficient method for the surface functionalization of nanoparticles with NIR hydrophobic fluorophores has been described. Surface loading of the hydrophobic fluorophores results in highly efficient fluorescence quenching in aqueous media which defines a particle off state. Particle fluorescence can be established in aqueous media in response to various surfactants. This off/on fluorescence responsive behavior has been extrapolated into a real-time biological imaging domain in which the cellular uptake of the particles with inclusion within organelles mimics the off/on switching obtained with surfactants. The ability of these fluorescence responsive nanoconstructs to allow real-time continuous imaging of their uptake into cells has been demonstrated in a movie format. Further targeted cellular imaging and diagnostic applications are currently being developed as is the expansion of our concepts to real-time *in vivo* imaging. As illustrated above different cell types show different responses to the same particles. As such a systematic response study of particle size, concentration, and surface fluorophore for different cell types is ongoing. The results from these studies will be reported in due course.

■ ASSOCIATED CONTENT

Supporting Information. Experimental methods, supporting figures, and real-time cellular uptake movies. This material is available free of charge via the Internet at http://pubs.acs.org.

■ AUTHOR INFORMATION

Corresponding Author
donal.f.oshea@ucd.ie

■ ACKNOWLEDGMENT

The authors acknowledge financial support from Science Foundation Ireland and the donation of nanoparticles from Varian Inc. M.G. thanks IRCSET for funding. Thanks are extended to the CSCB Mass Spectrometry and NMR Centres and the Conway Institutes imaging facilities.

■ REFERENCES

(1) Escobedo, J. O.; Rusin, O.; Lim, S.; Strongin, R. M. *Curr. Opin. Chem. Biol.* **2010**, *14*, 64–70.
(2) Ntziachristos, V.; Ripoll, J.; Wang, L. V.; Weissleder, R. *Nat. Biotechnol.* **2005**, *23*, 313–320.
(3) Weissleder, R.; Pittet, M. J. *Nature* **2008**, *452*, 580–589.
(4) Frangioni, J. V. *J. Clin. Oncol.* **2008**, *26*, 4012–4021.
(5) Razansky, D.; Distel, M.; Vinegoni, C.; Ma, R.; Perrimon, N.; Köster, R. W.; Ntziachristos, V. *Nature Phot.* **2009**, *3*, 412–417.
(6) (a) White, A. G.; Fu, N.; Leevy, W. M.; Lee, J.-L.; Blasco, M. A.; Smith, B. D. *Bioconjugate Chem.* **2010**, *21*, 1297–1304. (b) Yang, Y.; Lowry, M.; Xu, X.; Escobedo, J. O.; Sibrian-Vazquez, M.; Wong, L.; Schowalter, C. M.; Jensen, T. J.; Fronczek, F. R.; Warner, I. M.; Strongin, R. M. *Proc. Natl. Acad. Sci. U.S.A.* **2008**, *105*, 8829–8834.
(7) Trivedi, E. R.; Harney, A. S.; Olive, M. B.; Podgorski, I.; Moin, K.; Sloane, B. F.; Barrett, A. G. M.; Meade, T. J.; Hoffman, B. M. *Proc. Natl. Acad. Sci. U.S.A.* **2010**, *107*, 1284–1288.
(8) (a) Tasior, M.; O'Shea, D. F. *Bioconjugate Chem.* **2010**, *21*, 1130–1133. (b) Gorman, A.; Killoran, J.; O'Shea, C.; Kenna, T.; Gallagher, W. M.; O'Shea, D. F. *J. Am. Chem. Soc.* **2004**, *126*, 10619–10631.
(9) Nguyen, Q. T.; Olson, E.; Aguilera, T. A.; Jiamg, T.; Scadeng, M.; Ellies, L. G.; Tsien, R. Y. *Proc. Natl. Acad. Sci. U.S.A.* **2010**, *107*, 4317–4322.
(10) Murtagh, J.; Frimannsson, D. O.; O'Shea, D. F. *Org. Lett.* **2009**, *11*, 5386–5389.
(11) Stark, W. J. *Angew. Chem., Int. Ed.* **2011**, *50*, 1242–1258.
(12) (a) He, X.; Wang, K.; Zhen Cheng, Z. *WIREs Nanomed. Nanobiotechnol.* **2010**, *2*, 349–366. (b) Rungta, P.; Bandera, Y. P.; Roeder, R. D.; Li, Y.; Baldwin, W. S.; Sharma, D.; Sehorn, M. G.; Luzinov, I.; Foulger, S. H. *Macromol. Biosci.* **2011**, *11*, 927–937.
(13) Solution aggregates of molecular fluorophores are known to present different photophysical properties to their deaggregrated molecules with fluorescence quantum yield often being one of the most pronounced differences; for examples, see: Chen, Z.; Lohr, A.; Saha-Möller, C. R.; Würthner, F. *Chem. Soc. Rev.* **2009**, *38*, 564–584.
(14) Maldiney, T.; Richard, C.; Seguin, J.; Wattier, N.; Bessodes, M.; Scherman, D. *ACS Nano* **2011**, *5*, 854–862.
(15) Li, M.; Rharbi, Y.; Huang, X.; Winnik, M. A. *J. Colloid Interface Sci.* **2000**, *230*, 135–139.
(16) This does not preclude TX-100−particle interactions at concentrations lower than the CMC though they have a less significant impact on particle fluorescence.